Anomalous Fluctuations of Bose-Einstein Condensates in Optical Lattices

Zahra Jalali-Mola,[1] Niklas Käming,[2,3] Luca Asteria,[4] Utso Bhattacharya,[1,5] Ravindra W. Chhajlany,[6] Klaus Sengstock,[2,3] Maciej Lewenstein,[1,7] Tobias Grass,[8,9,*] and Christof Weitenberg[10,†]

[1]*ICFO—Institut de Ciencies Fotoniques, The Barcelona Institute of Science and Technology, 08860 Castelldefels, Barcelona, Spain*
[2]*Institute for Quantum Physics, University of Hamburg, 22761 Hamburg, Germany*
[3]*The Hamburg Centre for Ultrafast Imaging, 22761 Hamburg, Germany*
[4]*Department of Physics, Graduate School of Science, Kyoto University, Kyoto 606-8502, Japan*
[5]*Institute for Theoretical Physics, ETH Zurich, Zurich, Switzerland*
[6]*Institute of Spintronics and Quantum Information, Faculty of Physics, Adam Mickiewicz University, 61-614 Poznań, Poland*
[7]*ICREA, Passeig de Lluís Companys 23, 08010 Barcelona, Spain*
[8]*DIPC—Donostia International Physics Center, Paseo Manuel de Lardizábal 4, 20018 San Sebastián, Spain*
[9]*Ikerbasque—Basque Foundation for Science, Maria Diaz de Haro 3, 48013 Bilbao, Spain*
[10]*Department of Physics, TU Dortmund University, 44227 Dortmund, Germany*

(Received 4 August 2025; revised 5 November 2025; accepted 12 December 2025; published 23 February 2026)

Fluctuations are fundamental in physics and important for understanding and characterizing phase transitions. In this spirit, the phase transition to the Bose-Einstein condensate (BEC) is of specific importance. Whereas fluctuations of the condensate particle number in atomic BECs have been studied in continuous systems, experimental and theoretical studies for lattice systems were so far missing. Here, we explore the condensate particle number fluctuations in an optical lattice BEC across the phase transition in a combined experimental and theoretical study. We present both experimental data using ultracold ^{87}Rb atoms and numerical simulations based on a hybrid approach combining the Bogoliubov quasiparticle framework with a master equation analysis for modeling the system. We find strongly anomalous fluctuations, where the variance of the condensate number $\delta N_{\mathrm{BEC}}^2$ scales with the total atom number as $N^{1+\gamma}$ with an exponent around $\gamma_{\mathrm{theo}} = 0.74(10)$ and $\gamma_{\mathrm{exp}} = 0.62(9)$, which we attribute to the 2D/3D crossover geometry. Our Letter highlights the importance of the trap geometry on the character of fluctuations and on fundamental quantum mechanical properties.

DOI: 10.1103/95pq-6r5g

Introduction—Fluctuations are fundamental to the structure of physical reality. They provide information about the behavior of systems at different scales, from the quantum realm [1] to the cosmos [2], and are essential for both the theoretical understanding and practical applications of physics. The fluctuation-dissipation theorem establishes a deep connection between the fluctuations in a system at equilibrium and its response to external perturbations [3]. Fluctuations near critical points can drive phase transitions, creating ordered phases of matter through a mechanism known as order by disorder [4–7]. A test bed for studying fluctuations in a quantum system are atomic Bose-Einstein condensates in which a macroscopic number of bosonic particles accumulate in the ground state. This phase of matter, predicted in 1925, was for atomic gases first experimentally realized 70 years later, using magnetic traps to confine and cool alkali atoms to extremely low temperatures [8,9]. While conceptually simple, the condensate features interesting behavior, such as long-range phase coherence or superfluid flow [10]. The number fluctuations of Bose-Einstein condensates exhibit particularly subtle properties that have spurred theoretical discussions and investigations for many decades; see the review articles in Refs. [11,12]. More recently, fluctuations in atomic Bose-Einstein condensates have also become the subject of experimental investigations [13–15].

Notably, even in the theoretically most tractable case of an ideal Bose gas, the number fluctuations of the condensate behave in a very intriguing way: different thermodynamic ensembles strongly disagree regarding the amount of fluctuations in a noninteracting gas [11,16–20], while being consistent regarding the mean value of the condensate fraction. The grand-canonical ensemble exhibits a particularly dramatic behavior, which is often referred to as the grand-canonical catastrophe: condensate fluctuations δN_{BEC} are of the order of the particle number N [16]. In contrast, the microcanonical and canonical ensembles yield

[*]Contact author: tobias.grass@dipc.org
[†]Contact author: christof.weitenberg@tu-dortmund.de

the same amount of fluctuations in 1D [18,19], whereas in a 3D trapped gas, the two ensembles agree only with respect to the scaling behavior, and the absolute amount of fluctuations is suppressed in the microcanonical ensemble [17,21]. The suppression of fluctuations in the microcanonical ensemble has also been seen experimentally [14]. The condensation of photons [22,23] has opened the door toward experimental investigation of the scenario given by an ideal gas in the grand-canonical ensemble, realized by an effective particle exchange between the photon gas and a dye reservoir by absorption and emission processes, although the finite size of the dye reservoir needs to be taken into account. The grand canonical BEC fluctuations have been measured in this system via second order coherence of the photons [24].

Apart from the grand-canonical catastrophe, the scaling of the condensate number fluctuations with the system size is found to deviate from Gaussian behavior $\delta N^2_{\mathrm{BEC}} \propto N$ also in other ensembles. In this context, a tremendously important role is played by the geometry of the system. In a box-shaped potential, the single-particle energies $\epsilon_i \propto k_i^\sigma$ disperse quadratically, $\sigma = 2$, whereas in a harmonic trap potential the dispersion is linear, $\epsilon_i \propto n_i^\sigma$ with $\sigma = 1$, where k_i and n_i denote the quantum numbers in the respective geometry. Together with the dimensionality d of the system the dispersive behavior σ has crucial consequences on the phenomenon of Bose-Einstein condensation [12,21,25], and in particular on the scaling of condensate fluctuations: While for $d < \sigma$ condensation does not even occur at all, the condensate of ideal bosons exhibits normal fluctuations for $d > 2\sigma > 0$, with a scaling behavior $\delta N^2_{\mathrm{BEC}} \propto N\tilde{T}^{d/\sigma}$ at low temperature, where $\tilde{T} = T/T_{\mathrm{c}}$ denotes reduced temperature, that is, the temperature T in units of the critical temperature T_{c}. Such scenario corresponds, for instance, to a 3D Bose gas in a harmonic trap. In contrast to this, for $\sigma < d < 2\sigma$, the scaling of fluctuation is anomalous, $\delta N^2_{\mathrm{BEC}} \propto N^{2\sigma/d}\tilde{T}^2$. Accordingly, for the 3D box potential, the scaling is $\delta N^2_{\mathrm{BEC}} \propto N^{1+\gamma}$ with an an exponent $\gamma = 1/3$ [26].

For the interacting Bose gas, the scaling behavior of fluctuations has given rise to controversial results, as exact results for interacting systems are not available, and the predictions sensibly depend on the chosen approximations [27] and finite-size effects. For instance, the Bogoliubov treatment [26] as well as number-conserving approaches [28,29] predict anomalous scaling for a harmonically trapped 3D gas, whereas a perturbative approach found normal scaling [30]. Reference [31] has argued that anomalous scaling in the Bogoliubov approach is due to inconsistent higher-order terms. For a recent review of this controversy, see also Ref. [12]. Experiments with interacting ultracold atoms in an elongated 3D harmonic trap found a scaling exponent of $\gamma = 0.134(5)$ [14], which is reduced compared to the prediction $\gamma = 1/3$ for the interacting gas in the 3D harmonic trap [26,32] due to the dimensional effect of the elongated trap.

In contrast to the vast amount of literature on condensate fluctuations in continuous systems, very little attention has been paid to lattice systems [33], despite the general great importance of optical lattices for ultracold atoms [34]. The present Letter closes this gap of knowledge, and investigates, both experimentally and theoretically, the case of bosonic atoms in an optical lattice potential. In addition, a three-dimensional (3D) harmonic trap potential confines the atoms, with the trap along the perpendicular direction being much weaker than within the lattice plane. This combination of traps gives rise to a triangular array of tubes, as illustrated in Fig. 1(b). A BEC in an array of tubes was shown to exhibit the physics of 2D systems concerning vortex proliferation and short-range coherence [35,36] but the behavior of condensate fluctuations in such geometry, also known as 2D/3D crossover, has not been studied. Here we show that such a system exhibits strongly anomalous scaling of the condensate fraction fluctuations with the particle number. On the experimental side, we use a matter-wave microscope for precision thermometry from high-resolution density measurements of ultracold ^{87}Rb atoms [37] allowing to extract the condensate fraction for each image. On the theory side, we use a hybrid approach

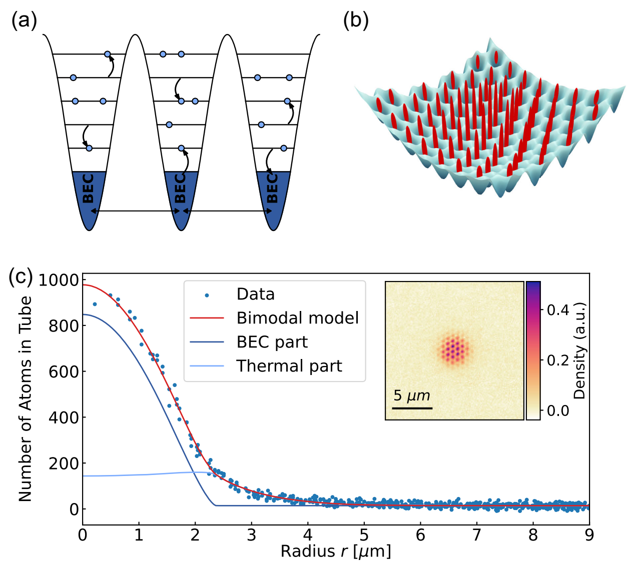

FIG. 1. Trap geometry and density profiles of the BECs. (a) The fluctuations arise due to continuous particle exchange between different energy levels. (b) The trap geometry consists of a triangular lattice of tubes within a harmonic confinement. (c) Radial density profile of tube occupations of a typical BEC along with the fitted bimodal distribution, consisting of the density of the BEC n_{BEC} and the density of the thermal cloud n_{th}. The inset shows the density observed with the matter-wave microscope. This image was obtained for an evaporation frequency $f_{\mathrm{evap}} = 95.0$ kHz and yields fit parameters of BEC particle number $N_{\mathrm{BEC}} = 13300 \pm 150$, fugacity $z = 2.13 \pm 0.14$, temperature $T = 115 \pm 3$ nK, and overall particle number $N_{\mathrm{tot}} = 24100 \pm 600$.

combining the Bogoliubov quasiparticle framework with a master equation analysis [28,38–41]. We find $\gamma_{\text{theo}} = 0.74(10)$ for the numerics and $\gamma_{\text{exp}} = 0.62(9)$ for the experimental data. These values match well, and they are in between the expected values for non-interacting systems with the density of states of a truly 2D lattice ($\gamma = 1$) and a truly 3D lattice ($\gamma = 1/3$) [11]. The fluctuations follow a curve as a function of the reduced temperature, which has a pronounced peak below T_c, which further shifts down with increasing interactions.

Experimental setup—Our experiments start with BECs of ^{87}Rb atoms prepared in a magnetic trap in the $F = 2, m_F = 2$ state. The trap is radially symmetric in the x, y plane with a high trapping frequency of $\omega_{xy} = 2\pi \times 305$ Hz and a trapping frequency of $\omega_z = 2\pi \times 29$ Hz in the z direction. We load into a triangular optical lattice formed by lattice beams with a wavelength of $\lambda = 1064$ nm, yielding a lattice constant $a_{\text{lat}} = 2\lambda/3 = 709$ nm, and the recoil energy $E_{\text{rec}} = (h^2/2m\lambda^2)$ with Planck's constant h and the atomic mass m. We work with a lattice depth of $1E_{\text{rec}}$ [37,42], which yields a tunneling energy of $J = h \times 12$ Hz.

To map out the phase transition, we prepare the system at different temperatures and atom numbers by varying the end point of the radio-frequency evaporation ramp in the magnetic trap before the loading into the lattice between 95 and 119 kHz, with the resonance frequency to the $m_F = 1$ state being $\lesssim$90 kHz. For high-resolution imaging of the real-space profiles with single-tube resolution, we employ the matter-wave microscope technique described in [37,43]. We first ramp the lattice to $6E_{\text{rec}}$ ($J/h \sim 10^{-3}$ Hz) to freeze the density distribution and wait for 12 ms to let the system dephase, in order to avoid interaction effects during the matter-wave protocol due to density peaks. We then ramp the in-plane trap frequency to $\omega_{\text{pulse}} = 2\pi \times 390$ Hz for a large matter-wave magnification of 44. The protocol consists of a quarter-period pulse in the harmonic trap initialized by switching off the optical lattice and a subsequent free evolution by 18 ms. Finally, we perform absorption imaging with an optical magnification of 2 on a CCD camera.

We determine the atom number, temperature and condensate fraction from each experimental image by fitting a semi-ideal bimodal model [44] to the density profiles, integrated over the Wigner-Seitz cells [Fig. 1(c) inset]. The bimodal fit contains the BECs fraction and the thermal fraction as well as the repulsive interaction of the BEC onto the thermal gas. We note that the high-resolution imaging of the density distribution via the matter-wave microscope allows precision thermometry of single images and precise modeling of the condensate fraction. This enables us to study the BEC fluctuations without the stabilization of the atom number using nondestructive imaging near the end of the evaporation ramp as in Refs. [13,14]. Technical fluctuations of the prepared atom number do not impede our analysis and the statistical error on the obtained condensate fraction from the fit is smaller than the measured shot-to-shot fluctuations, which we therefore attribute to physical fluctuations of the BEC. The typical atom number at the peak of the fluctuations at $T/T_c^0 = 0.65$ is around 30 000 atoms.

We model the density distribution as a continuous system with a modified interaction constant g given by $g_{\text{eff}} = gA_{\text{WS}}/(2\pi\sigma^2)$ with the area of the Wigner Seitz cell A_{WS} and the harmonic oscillator length σ on the lattice sites [37].

Theoretical method—In order to theoretically describe the system, we employ the following Hamiltonian:

$$H = -J \sum_{<i,j>,f} (\hat{a}^{\dagger}_{i,f}\hat{a}_{j,f} + \text{H.c.}) + \sum_{i,f} V_{i,f}\hat{n}_{i,f} + \frac{U}{2}\sum_{i,f}\hat{n}_{i,f}(\hat{n}_{i,f} - 1), \quad (1)$$

where $\hat{a}^{\dagger}_{i,f}$ and $\hat{a}_{i,f}$ are the creation and annihilation operators at site i in mode f, $\hat{n}_{i,f} = a^{\dagger}_{i,f}a_{i,f}$ is the number operator, and $\langle i,j \rangle$ denotes nearest neighbor sites. Hamiltonian parameters are the single-particle tunneling J, the Bose-Hubbard interaction U, and the harmonic trapping potential, $V_{i,f} = V_{\text{t}}(x_i^2 + y_i^2) + f\hbar\omega_z$. Here, (x_i, y_i) are the spatial coordinates of site i in the xy plane, and the strength of the trap is given by $V_{\text{t}} = m\omega^2 a_{\text{lat}}^2/2 = 16.7J$. The different modes f are eigenmodes of the perpendicular trapping potential $V_{z,i} = m\omega_z^2 z^2/2$. For the perpendicular trapping frequency, we choose $\hbar\omega_z/J = 2.41$, to match the experimental conditions.

To analyze the system, we use the time-dependent Gross-Pitaevskii equation (GPE), which can be derived from the Heisenberg equation of motion applied to the second quantized Hamiltonian [46,47]. Following the idea of the decomposition of the field operators into the classical field, describing the Bose condensation, and fluctuation part determining the quantum excitations, $\hat{a}_{i,f}(t) \simeq (\Phi_{i,f} + \tilde{\psi}_{i,f}(t))e^{-i\epsilon_0 t/\hbar}$ with $\Phi_{i,f} = \langle \hat{a}_{i,f}(t) \rangle$, beside applying the Hartree-Fock-Bogoliubov (HFB) approximation and mean-field theory, we can derive the two coupled equations corresponding to the stationary GPE and the excitation particles. The derivation follows standard techniques as outlined in Refs. [48–50] and references therein:

$$(V_{i,f} - \epsilon_0)\Phi_{i,f} - J\sum_{<j>}\Phi_{j,f} + U(n^c_{i,f}\Phi_{i,f} + 2\Phi_{i,f}\tilde{n}_{i,f} + \Phi^{\dagger}_{i,f}\tilde{\Delta}_{ii,f}) = 0, \quad (2)$$

$$i\frac{d\tilde{\psi}_{i,f}}{dt} = -\sum_{<j>}J\tilde{\psi}_{j,f} + [V_{i,f} - \epsilon_0 + 2U(n^c_{i,f} + \tilde{n}_{i,f})]\tilde{\psi}^{\dagger}_{i,f} + U(\Delta^{c*}_{ii,f} + \tilde{\Delta}^{*}_{ii,f})\tilde{\psi}_{i,f}. \quad (3)$$

Here, at each lattice site i, we define the number of particles in the condensate as $n^c_{i,f} = |\Phi_{i,f}|^2$, the condensate pairing as $\Delta^c_{ii,f} = \Phi^2_{i,f}$, the number of noncondensate particles as $\tilde{n}_{i,f} = \langle \tilde{\psi}^\dagger_{i,f} \tilde{\psi}_{i,f} \rangle$, and the pairing of noncondensed particles, as $\tilde{\Delta}_{ii,f} = \langle \tilde{\psi}_{i,f} \tilde{\psi}_{i,f} \rangle$. The latter so-called anomalous terms are neglected (the Popov approximation) in the following. The quantity ϵ_0 stands for ground state energy of the condensate particles, and it is assumed that the total particle number $N = \sum_{i,f} \tilde{n}_{i,f} + n^c_{i,f}$ remains fixed. The two equations Eqs. (2) and (3) for the condensate and excited particles, respectively, are solved self-consistently yielding also the quasiparticle excitation spectrum and states.

We thus obtain the condensation fraction and analyze it below as function of the number of particles in the system. In order to study fluctuations of the condensate, one needs to obtain the fluctuations of the non condensed particles from which the ground state fluctuations can be inferred. However, it is known that the Bogoliubov-Popov approximation breaks down at intermediate temperatures (close to the critical temperature). Since we are interested in the description of a system with fixed particle number and over a wide range of temperatures, we employ therefore a hybrid method combining the Bogoliubov approach with the master equation method introduced in [11,39–41] that was shown to yield well behaved predictions for condensate fluctuations even across T_c. In this approach, the noncondensed particles act as a reservoir that facilitates the thermalization of the condensate [by exciting particles from the condensate through the absorption of Bogoliubov quasi-particles and vice versa; see Fig. 1(a)]. A master equation for the condensate is then obtained which depends on the statistical properties of the Bogoliubov quasiparticles which are available from the solution of Eq. (3). The master equation technique introduces thermal corrections to the condensate fluctuations (see Sec. 2.3 of Supplemental Material [44]).

Results—We start by comparing the condensate fraction as a function of reduced temperature of the experiment and the numerics for $N = 1000$ particles (Fig. 2). Both curves show a smooth function resulting from the finite system size. We repeat the numerics for different interaction strength between $U = 0$ and $U = 0.1J$ and find an expected shift of the critical temperature to smaller values [48]. The range of interaction strengths fits with an estimate of the effective Hubbard interactions in the experiment [51], which is $U/J = 0.18$ for a central tube with 1000 atoms and correspondingly less in the outer tubes and for smaller total atoms numbers. In comparison to a continuous trap with the same scattering length, the interactions are enhanced by a factor 5, which makes the semiideal model necessary and which is responsible for the larger shift of the fluctuation peak compared to Ref. [13]. We note that the curves from numerical and experimental data match

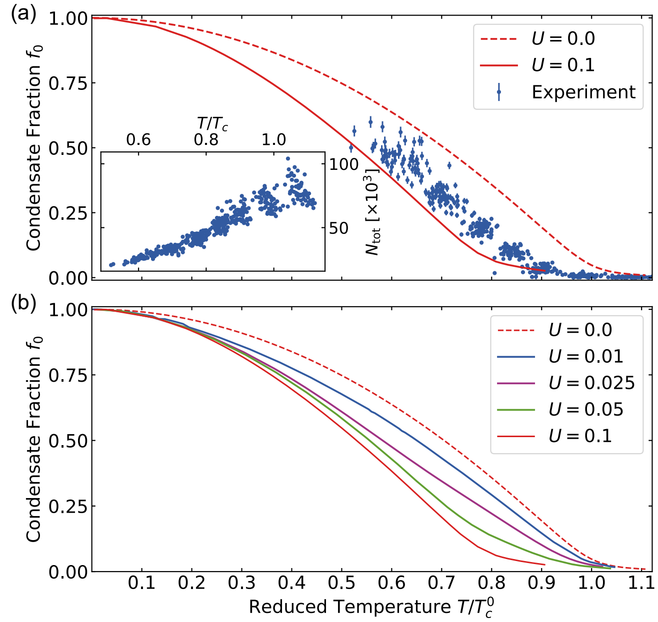

FIG. 2. Condensate fraction across the phase transition for the interacting system. Numerical results for a fixed particle number $N = 1000$ for the non interacting case (dashed red line) and the interacting case (solid red line) together with the experimental results (blue dots). Here, temperature is scaled by the non interacting temperature T^0_c [44]. The experimental data show the values extracted from individual images and indicate strong fluctuations. The clustering of the data points is due to the finite steps of the final evaporation frequency in the preparation. The inset shows the influence of varying Hubbard interaction strength $U/J = 0.0$, 0.01, 0.025, 0.05, 0.1 in the numerics.

although the experiment has around 30 times more particles. This is to be expected, because the numerics shows that the condensate fraction becomes relatively independent of atom number and interactions at large $N > 500$ and that the atom number dependence is well captured by the scaling relations.

Next, we compare the condensate fluctuations as a function of reduced temperature (Fig. 3). We find curves with a peak of the fluctuations at a temperature that shifts with interaction strength and reaches approximately $T \sim 0.65T^0_c$ for the interaction strength $U/J = 0.1$. In the numerics, we determine the scaling with atom number by varying the atom number while keeping all other parameters fixed and fitting $\delta N^2_{\mathrm{BEC}} \propto N^{1+\gamma}$. We find strongly anomalous scaling with an exponent $\gamma_{\mathrm{theo}} = 0.74(10)$, which is approximately independent of temperature in the absence of interactions. The systematic error stems from the residual temperature dependence in the experimentally relevant range (see End Matter). The same value holds for interacting systems irrespective of the interaction strength at sufficiently large temperature. Strong finite-size deviations are observed at low temperature, where γ sensibly depends on the interaction strength; see also the figures and their discussion in End Matter.

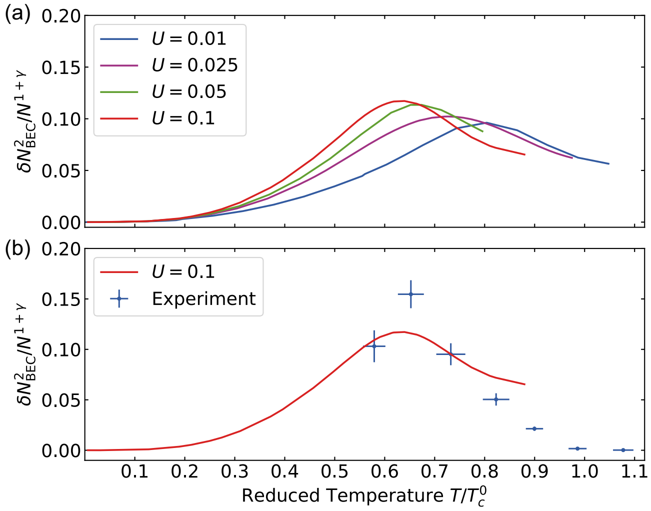

FIG. 3. Condensate fluctuation across the phase transition. (a) Variance of the condensate particle number from the numerics normalized by the total atom number $N = 1000$ with the anomalous scaling exponent $\gamma_{\text{theo}} = 0.74(10)$. When the Hubbard interaction strength is increased from $U/J = 0.01$ to $U/J = 0.1$, the peak of the fluctuations shifts from $T/T_c^0 = 0.8$ to $T/T_c^0 = 0.65$. (b) Variance of the condensate particle number in the experimental data (blue points) together with the numerics for $U/J = 0.1$ (solid line). The data agrees well for an experimental scaling exponent $\gamma_{\text{exp}} = 0.62(9)$, which is close to the theoretical value. The theory curves do not bend down at high temperatures, because the approach becomes less reliable close to the phase transition.

In the experiment, the temperature and atom number are correlated, because we vary the temperature by different end points of the evaporation ramp. We therefore extract the exponent of the anomalous fluctuations by considering the overall shape of the fluctuation curve as a function of the temperature normalized to the atom-number dependent critical temperature of the noninteracting system. We compare the curve of the theoretical fluctuation data normalized by $1/N^{1+\gamma_{\text{theo}}}$ with the experimental fluctuation data normalized by $1/N^{1+\gamma_{\text{exp}}}$ and find the best agreement for $\gamma_{\text{exp}} = 0.62(9)$, where the systematic error is the quadratic sum of the systematic error from the uncertainty of the atom number calibration of 10% and the systematic uncertainty inherited from the uncertainty of γ_{theo} (see Supplemental Material [44]). We thus find a consistent description with a mismatch of less than 20% between γ_{theo} and γ_{exp}, which gives evidence to establish these strongly anomalous fluctuations for our 2D/3D crossover geometry. We note that the exponents are in between the expected values for non-interacting systems in a truly 2D lattice ($\gamma = 1$) and a truly 3D lattice ($\gamma = 1/3$).

Conclusions—In conclusion, we have studied the condensate fluctuations of an interacting BEC in a triangular lattice of tubes both experimentally and theoretically and found strong anomalous scaling with the atom number with an exponent of $\gamma_{\text{theo}} = 0.74(10)$ and $\gamma_{\text{exp}} = 0.62(9)$. Our finding of anomalous fluctuations in large systems sizes of 30,000 atoms is an important contribution to the debate of anomalous scaling in the thermodynamic limit [11,12]. In the future, it would be interesting to study the BEC fluctuations in an atomic cloud, which thermalizes with a heat bath of a second species or where losses are introduced [52] or for BECs in higher bands of an optical lattice [53]. The study could be extended to full counting statistics [54], e.g., after an interaction quench [55]. Moreover, local fluctuations [56] or higher moments of the distributions [57] also provide valuable insights into BECs. The role of interactions on the condensate fluctuations is not fully understood and more studies are required, also including dipolar interactions. A detailed understanding of condensate fluctuations will become important in quantum metrology, e.g., for producing entangled atom pairs in atom interferometers via density dependent processes [58].

Acknowledgments—We thank Marcel Kosch, Henrik Zahn and Moritz Sträter for contributions in an early stage of the project. This work was funded by Deutsche Forschungsgemeinschaft (DFG, German Research Foundation) via Research Unit FOR 5688, Project No. 521530974, and via the cluster of excellence AIM, EXC 2056—Project ID 390715994 as well as by "Hamburg Quantum Computing," financed by the City of Hamburg and the European Union. U. B. acknowledges financial support of the IBM Quantum Researcher Program. R. W. C. acknowledges support from the Polish National Science Centre (NCN) under Maestro Grant No. DEC-2019/34/A/ST2/00081. T. G. acknowledges funding by the Department of Education of the Basque Government through the IKUR Strategy, through BasQ (project EMISGALA), and through PIBA_2023_1_0021 (TENINT), as well as by the Agencia Estatal de Investigación (AEI) through Proyectos de Generación de Conocimiento PID2022-142308NA-I00 (EXQUSMI), and that this work has been produced with the support of a 2023 Leonardo Grant for Researchers in Physics, BBVA Foundation. The ICFO-QOT group acknowledges support from the European Research Council AdG NOQIA; MCIN/AEI (PGC2018-09/10.13039/501100011033, CEX2019-000910- S/10.13039/501100011033, Plan National FIDEUA PID2019–106901 GB-I00, Plan National STAMEENA PID2022-139099NB-I00, project funded by MCIN/AEI/10.13039/501100011033 and by the "European Union NextGenerationEU/PRTR" (PRTR-C17.I1), FPI); QUANTERA DYNAMITE PCI2022- 132919, QuantERA II Programme cofunded by the European Union's Horizon 2020 program under Grant Agreement No. 101017733; Ministry for Digital Transformation and Civil Service of the Spanish Government through the QUANTUM ENIA project call—Quantum Spain project, and by the European Union through the Recovery, Transformation and Resilience

Plan—NextGenerationEU within the framework of the Digital Spain 2026 Agenda; MICIU/AEI/10.13039/501100011033 and EU (PCI2025-163167); Fundació Cellex; Fundació Mir-Puig; Generalitat de Catalunya (European Social Fund FEDER and CERCA program; Barcelona Supercomputing Center MareNostrum (FI-2023-3-0024); and the European Union (HORIZON-CL4-2022-QUANTUM-02-SGA PASQuanS2.1, 101113690, EU Horizon 2020 FET-OPEN OPTOlogic, Grant No. 899794, QU-ATTO, 101168628). This project has received funding from the European Union's Horizon Europe research and innovation program under Grant Agreement No. 101080086—NeQST; and the ICFO Internal "QuantumGaudi" project.

The BBVA Foundation is not responsible for the opinions, comments, and contents included in the project and/or the results derived therefrom, which are the total and absolute responsibility of the authors. Views and opinions expressed are however those of the author(s) only and do not necessarily reflect those of the European Union, European Commission, European Climate, Infrastructure and Environment Executive Agency (CINEA), or any other granting authority. Neither the European Union nor any granting authority can be held responsible for them.

The authors declare no competing financial interests.

Data availability—The data that support the plots presented in this Letter and other findings of this study are available from the corresponding author upon reasonable request.

[1] M. Campisi, P. Hänggi, and P. Talkner, Rev. Mod. Phys. **83**, 771 (2011).
[2] E. R. Harrison, Rev. Mod. Phys. **39**, 862 (1967).
[3] R. Kubo, Rep. Prog. Phys. **29**, 255 (1966).
[4] J. Villain, R. Bidaux, J.-P. Carton, and R. Conte, J. Phys. France **41**, 1263 (1980).
[5] D. Bergman, J. Alicea, E. Gull, S. Trebst, and L. Balents, Nat. Phys. **3**, 487 (2007).
[6] A. M. Turner, R. Barnett, E. Demler, and A. Vishwanath, Phys. Rev. Lett. **98**, 190404 (2007).
[7] R. Barnett, S. Powell, T. Graß, M. Lewenstein, and S. Das Sarma, Phys. Rev. A **85**, 023615 (2012).
[8] M. H. Anderson, J. R. Ensher, M. R. Matthews, C. E. Wieman, and E. A. Cornell, Science **269**, 198 (1995).
[9] K. B. Davis, M. O. Mewes, M. R. Andrews, N. J. van Druten, D. S. Durfee, D. M. Kurn, and W. Ketterle, Phys. Rev. Lett. **75**, 3969 (1995).
[10] L. Pitaevskii and S. Stringari, *Bose-Einstein Condensation and Superfluidity* (Oxford University Press, New York, 2016).
[11] V. V. Kocharovsky, V. V. Kocharovsky, M. Holthaus, C. Raymond Ooi, A. Svidzinsky, W. Ketterle, and M. O. Scully, *Advances in Atomic, Molecular, and Optical Physics* (Academic Press, New York, 2006), pp. 291–411.
[12] M. B. Kruk, P. Kulik, M. F. Andersen, P. Deuar, M. Gajda, K. Pawłowski, E. Witkowska, J. J. Arlt, and K. Rzążewski, Rep. Prog. Phys. **88**, 106401 (2025).
[13] M. A. Kristensen, M. B. Christensen, M. Gajdacz, M. Iglicki, K. Pawłowski, C. Klempt, J. F. Sherson, K. Rzążewski, A. J. Hilliard, and J. J. Arlt, Phys. Rev. Lett. **122**, 163601 (2019).
[14] M. B. Christensen, T. Vibel, A. J. Hilliard, M. B. Kruk, K. Pawłowski, D. Hryniuk, K. Rzążewski, M. A. Kristensen, and J. J. Arlt, Phys. Rev. Lett. **126**, 153601 (2021).
[15] T. Vibel, M. B. Christensen, R. M. F. Andersen, L. N. Stokholm, K. Pawłowski, K. Rzążewski, M. A. Kristensen, and J. J. Arlt, J. Phys. B **57**, 195301 (2024).
[16] R. M. Ziff, G. E. Uhlenbeck, and M. Kac, Phys. Rep. **32**, 169 (1977).
[17] P. Navez, D. Bitouk, M. Gajda, Z. Idziaszek, and K. Rzążewski, Phys. Rev. Lett. **79**, 1789 (1997).
[18] M. Wilkens and C. Weiss, J. Mod. Opt. **44**, 1801 (1997).
[19] M. Holthaus, E. Kalinowski, and K. Kirsten, Ann. Phys. (N.Y.) **270**, 198 (1998).
[20] M. B. Kruk, D. Hryniuk, M. Kristensen, T. Vibel, K. Pawłowski, J. Arlt, and K. Rzążewski, SciPost Phys. **14**, 036 (2023).
[21] C. Weiss and M. Wilkens, Opt. Express **1**, 272 (1997).
[22] C. Weiss and J. Tempere, Phys. Rev. E **94**, 042124 (2016).
[23] A. Crisanti, A. Sarracino, and M. Zannetti, arXiv:2505.24228.
[24] J. Schmitt, T. Damm, D. Dung, F. Vewinger, J. Klaers, and M. Weitz, Phys. Rev. Lett. **112**, 030401 (2014).
[25] S. De Groot, G. J. Hooyman, C. A. Ten Seldam, and E. A. Guggenheim, Proc. R. Soc. A **203**, 266 (1950).
[26] S. Giorgini, L. P. Pitaevskii, and S. Stringari, Phys. Rev. Lett. **80**, 5040 (1998).
[27] H. Xiong, S. Liu, G. Huang, and Z. Xu, Phys. Rev. A **65**, 033609 (2002).
[28] V. V. Kocharovsky, M. O. Scully, S.-Y. Zhu, and M. S. Zubairy, Phys. Rev. A **61**, 023609 (2000).
[29] Z. Idziaszek, Phys. Rev. A **71**, 053604 (2005).
[30] Z. Idziaszek, M. Gajda, P. Navez, M. Wilkens, and K. Rzążewski, Phys. Rev. Lett. **82**, 4376 (1999).
[31] V. I. Yukalov, Laser Phys. Lett. **2**, 156 (2004).
[32] F. Meier and W. Zwerger, Phys. Rev. A **60**, 5133 (1999).
[33] K. Dutkiewicz, M. Płodzień, A. Rojo-Francàs, B. Juliá-Díaz, M. Lewenstein, and T. Grass, arXiv:2505.16885.
[34] M. Lewenstein, A. Sanpera, and V. Ahufinger, *Ultracold Atoms in Optical Lattices: Simulating Quantum Many-Body Systems* (OUP, Oxford, United Kingdom, 2012).
[35] V. Schweikhard, S. Tung, and E. A. Cornell, Phys. Rev. Lett. **99**, 030401 (2007).
[36] J. C. Brüggenjürgen, M. S. Fischer, and C. Weitenberg, arXiv:2410.10611.
[37] L. Asteria, H. P. Zahn, M. N. Kosch, K. Sengstock, and C. Weitenberg, Nature (London) **599**, 571 (2021).
[38] M. O. Scully, Phys. Rev. Lett. **82**, 3927 (1999).
[39] M. O. Scully and A. A. Svidzinsky, J. Mod. Opt. **53**, 2399 (2006).
[40] A. A. Svidzinsky and M. O. Scully, Phys. Rev. A **82**, 063630 (2010).
[41] A. A. Svidzinsky and M. O. Scully, Phys. Rev. Lett. **97**, 190402 (2006).

[42] M. N. Kosch, L. Asteria, H. P. Zahn, K. Sengstock, and C. Weitenberg, Phys. Rev. Res. **4**, 043083 (2022).

[43] S. Brandstetter, C. Heintze, P. Hill, P. M. Preiss, M. Gałka, and S. Jochim, Phys. Rev. Lett. **135**, 103401 (2025).

[44] See Supplemental Material at http://link.aps.org/supplemental/10.1103/95pq-6r5g for the experimental data pipeline and further theoretical considerations, which includes Ref. [45].

[45] C. J. Pethick and H. Smith, *Bose–Einstein Condensation in Dilute Gases* (Cambridge University Press, Cambridge, England, 2008).

[46] F. Dalfovo, S. Giorgini, L. P. Pitaevskii, and S. Stringari, Rev. Mod. Phys. **71**, 463 (1999).

[47] C. Gies and D. A. W. Hutchinson, Phys. Rev. A **70**, 043606 (2004).

[48] S. Giorgini, L. P. Pitaevskii, and S. Stringari, Phys. Rev. A **54**, R4633 (1996).

[49] A. Griffin, Phys. Rev. B **53**, 9341 (1996).

[50] K. Suthar, A. Roy, and D. Angom, Phys. Rev. A **91**, 043615 (2015).

[51] H. P. Zahn, V. P. Singh, M. N. Kosch, L. Asteria, L. Freystatzky, K. Sengstock, L. Mathey, and C. Weitenberg, Phys. Rev. X **12**, 021014 (2022).

[52] P. J. Paulino, I. Lesanovsky, and F. Carollo, Phys. Rev. Lett. **132**, 260402 (2024).

[53] G. Wirth, M. Ölschläger, and A. Hemmerich, Nat. Phys. **7**, 147 (2011).

[54] S. P. Rath and W. Zwerger, Phys. Rev. A **82**, 053622 (2010).

[55] D. X. Horváth and C. Rylands, Phys. Rev. A **109**, 043302 (2024).

[56] G. E. Astrakharchik, R. Combescot, and L. P. Pitaevskii, Phys. Rev. A **76**, 063616 (2007).

[57] J.-P. Bureik, G. Hercé, M. Allemand, A. Tenart, T. Roscilde, and D. Clément, Nat. Phys. **21**, 57 (2024).

[58] F. Anders, A. Idel, P. Feldmann, D. Bondarenko, S. Loriani, K. Lange, J. Peise, M. Gersemann, B. Meyer-Hoppe, S. Abend, N. Gaaloul, C. Schubert, D. Schlippert, L. Santos, E. Rasel, and C. Klempt, Phys. Rev. Lett. **127**, 140402 (2021).

End Matter

Fluctuations scaling analysis—In order to determine the scaling behavior of the number fluctuations in the condensate, we have obtained numerical data for different system sizes, interactions strengths, and temperatures using the hybrid approach further described in Supplemental Material Sec. 2.3 [44]. Here, we present this data and focus on its analysis.

We first plot the fluctuations as a function of temperature for three different interaction strengths ($U/J = 0$, 0.005, 0.01) in the three panels of Fig. 4. In each panel, we show fluctuations for different particle numbers N, normalized by $N^{1+\gamma}$, where γ is chosen such that the data variance at the peak is minimized. Slight dependence of γ on interactions U are noted, with the smallest value, $\gamma = 0.74$, for the noninteracting system, and the largest value $\gamma = 0.78$ for $U/J = 0.01$. We observe that (i) the scaling works well for system sizes $N > 500$, with data collapsing to a single peak value in all cases. For smaller systems, deviations are observed. (ii) The peak of the fluctuations is shifted to a lower temperature as interactions are increased. This shift is consistent with the interaction-induced depletion of the condensate, which reduces the temperature at which the maximum fluctuations are observed.

To further analyze this temperature dependence of the scaling, we have concentrated on the data for $N \geq 100$, and fitted it to a function $f(N) = c(T)N^{1+\gamma(T)}$ at each value of T. The obtained temperature-dependent fit parameters $c(T)$ and $\gamma(T)$, together with their error bars from the fitting error, are shown in Fig. 5. In its context, the following observations can be made: (i) the fit function accurately matches the data for all temperatures and for all interaction strengths. This is evidenced by tiny statistical error bars which (except for small T) are barely visible in the plots. We note that alternative fit functions, containing also

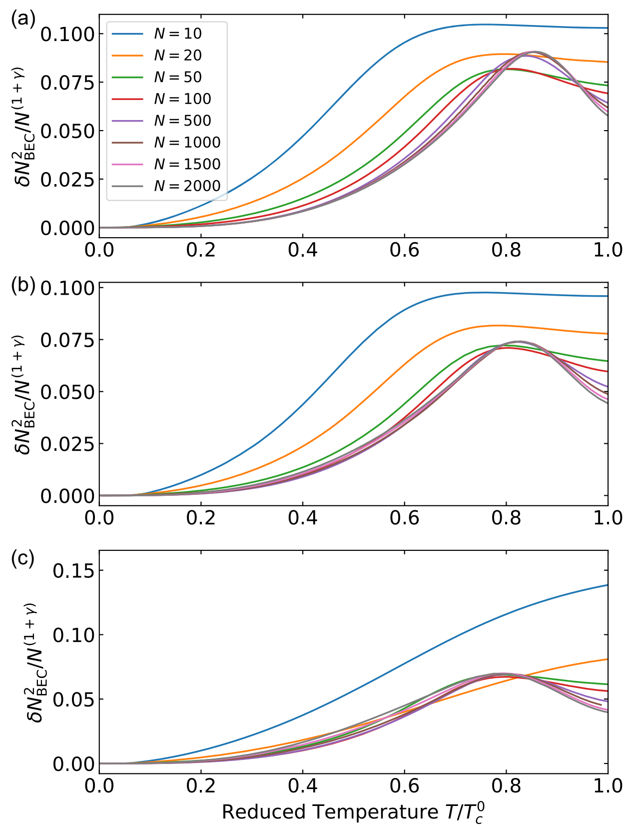

FIG. 4. Condensate Fluctuations vs. reduced temperature at various particle numbers, for (a) non-interacting gas, (b) interacting gas at $U/J = 0.005$, (c) interacting gas at $U/J = 0.01$. In all panels, the atom number fluctuations are scaled with particle number $N^{1+\gamma}$ and the scaling parameter is (a) $\gamma = 0.74$, (b) $\gamma = 0.77$, and (c) $\gamma = 0.78$, chosen such that the variance of the peak values is minimized in each panel. All numerical data has been obtained for trap parameters $\omega_z/J = 2.41$ and $V_{\mathrm{trap}}/J = 16.7$.

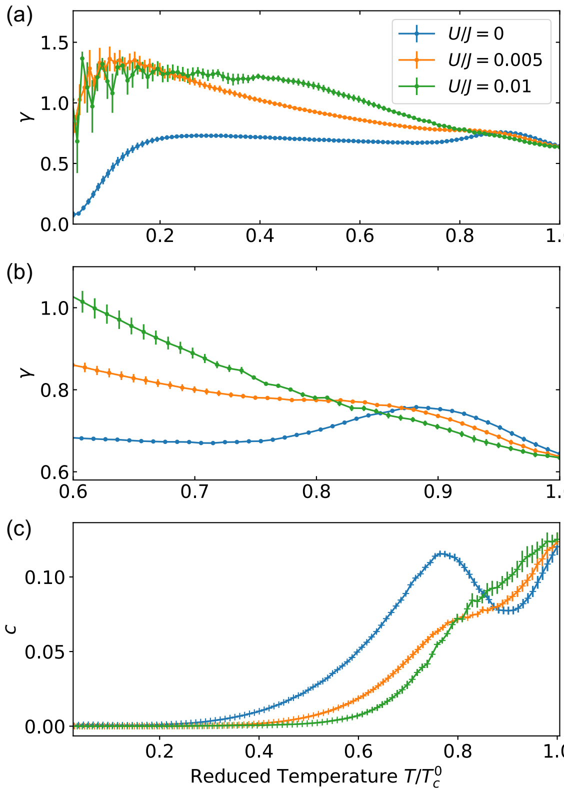

FIG. 5. Anomalous exponent of fluctuations extracted from numerical data with system sizes up to $N = 2000$. We show the fit parameters (a),(b) $\gamma(T)$, and (c) $c(T)$, obtained from matching the condensate fluctuation data at each temperature to the function $c(T)N^{1+\gamma(T)}$, for different interaction strengths: $U/J = 0$, 0.005, 0.01. A detailed view of the exponent at high temperature regime is shown in (b).

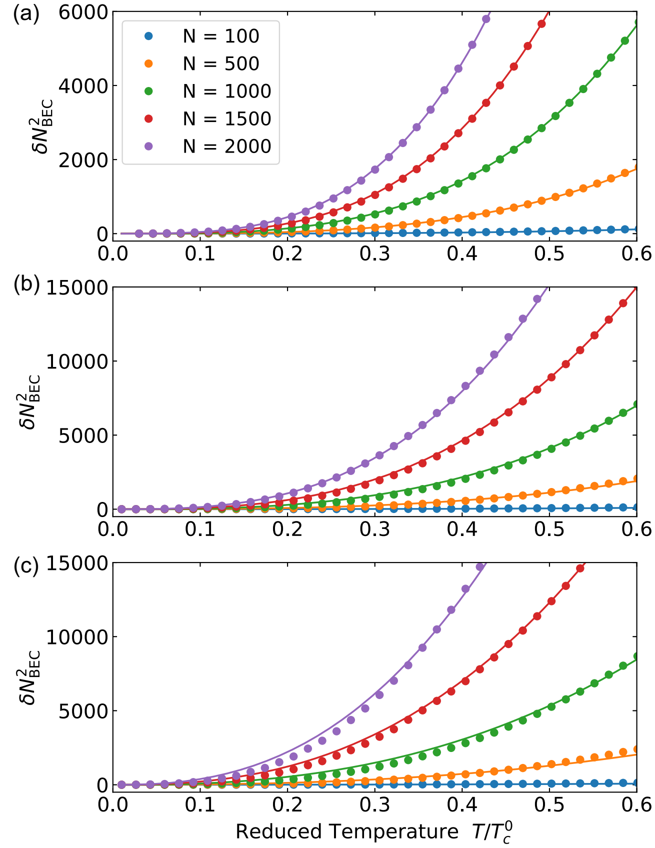

FIG. 6. Low temperature scaling of fluctuations with reduced temperature and particle number. We fit the numerical data to $cN^{(1+\gamma)}(T/T_c^0)^b$ with temperature-independent parameters c, γ, b. for (a) the noninteracting system $U/J = 0$, (b) the interacting system with $U/ = 0.005$, and (c) the interacting system with $U/J = 0.01$. We obtain (a) $c = 0.28$, $\gamma = 0.68$, $b = 3.37$, (b) $c = 0.07$, $\gamma = 0.88$, $b = 2.89$, and (c) $c = 0.02$, $\gamma = 1.05$, $b = 2.51$.

$\log(N)$ terms, have led to larger fit errors. (ii) At high temperatures between T/T_c^0 of 0.8 and 1.0 the exponent γ becomes approximately independent of the interaction strength U. We explain this by the very small condensate sizes at these high temperatures, which make interaction effects less important. This observation is particularly relevant for our comparison with experimental data, which is carried out in the high-temperature regime and hence does not depend on an accurate calibration of the interaction strength. We attribute a systematic error of 0.1 on a the $\gamma_{\rm theo} = 0.74$ derived for the peak fluctuations in the non-interacting system (see Fig. 4) stemming from this residual variation as a function of temperature and interaction strength in the relevant range.

At smaller temperature, the scaling parameter γ is increased by interactions. This trend can be understood by the fact that interactions deplete the condensate, thereby enhancing fluctuations. This observation highlights the significant role that interactions play in driving fluctuations within the condensate.

For an improved analysis of the low-temperature regime, we take advantage of the fact that at small T/T_c^0 the fluctuations exhibit a polynomial scaling in reduced temperature, and submit the entire data for $N \geq 100$ and T/T_c^0 below the peak temperature to a fit procedure $f(N, T/T_c^0) = c(T/T_c^0)^b N^{1+\gamma}$, with only three temperature-independent fit parameters. The result is shown in Fig. 6. At any U, the temperature scaling is approximately cubic. For the number scaling, we obtain values of γ between 0.68 (noninteracting case) and 1.05 ($U/J = 0.01$). This fit confirms the previously observed trend of interaction-increased γ at low temperatures.

In summary, our analysis predicts theory values for γ in the range between 0.7 and 1.1, depending on interaction strength and temperature. However, in the experimentally relevant high-temperature regime, this range is significantly smaller, $\gamma = 0.74 \pm 0.10$, used for the comparison with experiment in the relevant temperature range; see also Fig. S3 [44].